Optica Applicata, Vol. XLV, No. 1, 2015
DOI: 10.5277/oa150109

Enhancing light harvesting of organic solar cells by using hybrid microlenses

XIAO XIAO[1, 2, 3], ZHIYOU ZHANG[1, 3], SHIWEI XIE[1, 3], YU LIU[1, 3], DEJIAO HU[1, 3], JINGLEI DU[1, 3*]

[1]College of Physical Science and Technology, Sichuan University, Chengdu, 610064, China

[2]College of Physics and Electronic Engineering, Leshan Normal University, Leshan, 614000,China

[3]Key Laboratory of High Energy Density Physics and Technology of Ministry of Education, Sichuan University, Chengdu, 610064, China

[*]Corresponding author: dujl@scu.edu.cn

Organic solar cells have drawn intense attentions in recent years due to their inherent advantages. But the relatively low power conversion efficiency is the main obstacle in the way of organic solar cell commercialization. One of the main reasons that limit the power conversion efficiency is the mismatch between electrical transmission properties and light absorption properties in an organic active layer. In this work, a highly efficient light trapping scheme with a hybrid microlens array is proposed to resolve this contradiction. This structure can achieve broadband absorption enhancement in the spectrum of interest by chromatic aberration correction and hole parameter adjustment. And the light trapping element can be separated from cells to avoid direct contact with an organic layer that may cause electrical defects. Moreover, it is also compatible with low cost manufacturing technologies.

Keywords: organic solar cells, hybrid microlens, light harvesting, achromatization.

1. Introduction

As one of the promising renewable energy technologies, photovoltaic power has the low-cost potential to meet the growing energy demands of the expanding population and economic growth. Though silicon solar cells currently dominate the photovoltaic market, organic solar cells (OSCs) have drawn intense attentions in recent years due to their inherent advantages, including light weight, flexibility, and the possibility of inexpensively producing large-area devices. Therefore, OSCs are considered to be more suitable for building integrated photovoltaics than their inorganic competitors, and can open novel photovoltaic applications in many areas, such as integrated photo-

voltaic chargers for portable electronics, electronic textiles, synthetic skin and robotics, *etc*.

Though considerable advances have been made recently in device materials, structures, and manufacturing methods [1–4], the relatively low power conversion efficiency (PCE) is the main obstacle in the way of OSC commercialization. One of the main reasons that limit the PCE is the mismatch between electrical transmission properties and light absorption properties in an organic active layer, because organic semiconductors have inferior carrier mobility, and their exciton diffusion lengths ($L_D \sim 10$ nm) are far shorter than optical absorption lengths ($L_A \sim 100$ nm) in an organic active layer. The reduction in active layer thickness implies the loss of a large fraction of the incident light; conversely, the increase in active layer thickness leads to an increase in series resistance and reduction in carrier collection. So, it has to enforce a compromise between efficient light harvesting and efficient charge collection. In previous studies, researchers have proposed some light trapping structures to resolve this contradiction [5–11], such as plasmonic nanostructures, photonic crystals, diffraction gratings and so on. These structures essentially extend the thickness of an organic active layer, therefore the absorption enhancement equivalent to that of a much thicker layer is achieved, and nevertheless good electrical transport properties of a thin layer are retained. However, these structures usually suffer from several major drawbacks which impede their use in application, for example, the broadband absorption enhancement has not yet been achieved. Moreover, the complicated process may harm the soft organic layer and the quality of the devices, and is incompatible with standard technologies, which leads to high costs, *etc*.

In this work, we propose a highly efficient light-trapping scheme with hybrid microlenses for OSCs, which can enhance light harvesting in the spectrum of interest by chromatic aberration correction and hole parameter adjustment. In this trapping structure, each microlens is an achromatic hybrid refractive-diffractive singlet, which can be manufactured in one optical material, and these hybrid microlenses are separated from cells to avoid direct contact with an organic layer that may cause electrical defects. Moreover each microlens is also compatible with low cost manufacturing technologies such as imprint and lithography.

2. Light trapping system and materials

2.1. Light trapping system

As shown in Fig. 1, this light trapping system consists of three parts: a hybrid microlens array, a mirror with a hole array and an OSC with a reflecting cathode. Among the lens arrays, each hybrid microlens is the combination of a refractive lens and a diffractive lens. The refractive profile and the diffractive profile can thus be engraved on one surface. In addition, the mirror is located in the focal plane of the hybrid microlens array, and the holes in the mirror are especially placed in the focal spots. So the converging light which is collected by the lens array can propagate through those holes. As for the

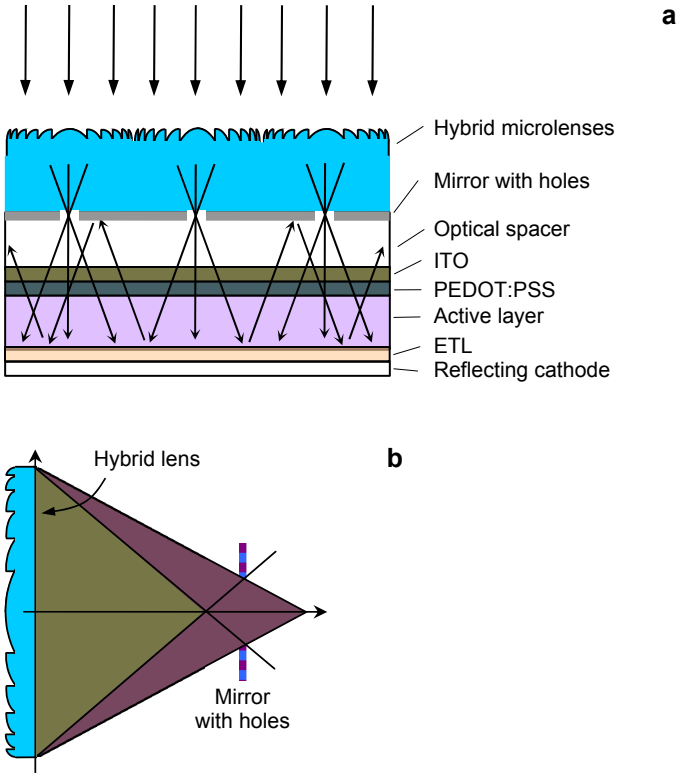

Fig. 1. Schematic illustration of an OSC with hybrid microlenses (**a**). Schematic diagram of a hybrid microlens and its achromatic analysis (**b**).

reflecting cathode in an OSC device, it has two functions, collecting photon-generated carriers and reflecting the light that is not being fully absorbed by the active layer. And apparently, the mirror and the reflecting cathode make up an optical reflection cavity.

Therefore, the basic concept of enhancing light harvesting is that the hybrid microlenses first collect incident collimated light, and then the convergent rays propagate through these small transmitting holes which locate at the focus spots of hybrid lenses. Finally, the transmission light bounces back and forth between the reflecting electrode of the OSC device and the mirror with holes. In other words, once light enter the optical reflection cavity, it would be confined and has small chance to escape from the cavity. Thus, multiple reflections inside the cavity can increase the effective optical path length in the active layer and the probability of photon absorption.

If hybrid lenses in this scheme are substituted by refractive lenses, perhaps this reduces the difficulty of manufacturing. But because of inevitable material dispersion, the larger longitudinal chromatic aberration (LCA) of refractive lenses will be obviously disadvantage to light harvesting [12–15]. Considering little difference in production cost between the two types of lenses, and that hybrid lenses can achieve more

excellent achromatism, the hybrid lens array is used to enhance light trapping in our scheme. A more detailed comparison between them will be introduced in Section 4.

Furthermore, a hybrid microlens array is unlike other light trapping structures, such as metal plasmonic structures, random textured surface, photonic crystals, diffraction gratings [7–11, 16] and so on. These structures either closely contact with soft active material or are embedded in an active layer, which may damage an organic active layer, resulting in electrical defects and short usage life. In this case (Fig. 1), the hybrid microlens array is separated from cells to avoid direct contact with the organic layer, so those negative effects mentioned above are avoided in our case.

2.2. Materials

In our design system, there is nothing special about the OSC element except the reflecting cathode (Fig. 1), and the conventional OSC has the following layer structure: ITO/hole transport layer (HTL)/organic active layer/electron transport layer (ETL)/Al. Usually, PEDOT:PSS or ZnO functions as HTL, TiO_x or LiF functions as ETL, and organic active material is P3HT:PCBM, MEH-PPV:PCBM, *etc*.

The hybrid microlens array is a key component of the proposed system and, as stated previously, it can be manufactured in one optical material and the whole lens profile can be engraved on one surface. In consideration of excellent light harvesting efficiency and ease duplication with a cost-efficient technology, the lens material must meet the following requirements: high transmittance and low dispersion in the absorption region of the active layer, low cost, and high impact resistance. Compared with glass, optical polymers which have these characteristics are preferred lens materials. Nowadays, poly(methyl methacrylates) (PMMA) is probably the most common optical polymer in plastic optics, which has high transmittance and low dispersion curve in the visible region. At the same time, the absorption spectrum of organic active materials is typical from 360 to 900 nm. This means that PMMA is very suitable for hybrid microlenses. Figure 2 shows dispersion curves of two PMMA samples [14, 17]. Because

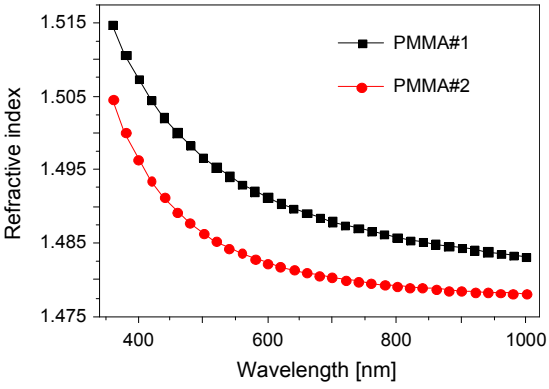

Fig. 2. Dispersion curves of PMMAs.

of similar trends of the curves in Fig. 2, only the refractive index data of PMMA#1 are applied to the simulation and discussion in this text.

3. Theory

3.1. Hybrid microlens

The hybrid singlet consists of a refractive microlens and a diffractive microlens, and the diffractive structure is fabricated on the surface of the refractive lens. For an ideal (with only chromatic aberration) plano-convex lens in air, the focal distance f_{ref} under the paraxial condition is given by the following equation:

$$f_{\mathrm{ref}}(\lambda) = \frac{R}{n(\lambda) - 1} \tag{1}$$

where R is the radius of curvature of the refractive lens, $n(\lambda)$ is the refractive index of the lens material.

An ideal diffractive lens (often call *kinoform*) only has one focus and a theoretical diffraction efficiency of 100% at a design wavelength λ_0 [15, 18]. The focal distance f_{dif} of a *kinoform* is given by

$$f_{\mathrm{dif}}(\lambda) = \frac{\lambda_0}{\lambda} f_{\mathrm{dif}}(\lambda_0) \tag{2}$$

The surface-relief structure of the ideal *kinoform* is piecewise continuous, each zone is designed to keep a constant optical path length to the focal point. Between two neighboring zones, the phase difference is 2π in order to create a continuity of the transmitted phase. This continuity is ensured by zones with a constant thickness h of a few micrometers

$$h = \frac{\lambda_0}{n(\lambda_0) - 1} \tag{3}$$

Since the diffractive relief structure is engraved on the surface of the refractive lens, the distance between the two lenses is zero. Therefore, the effective focal length f_{eff} of the hybrid lens is given by

$$\frac{1}{f_{\mathrm{eff}}(\lambda)} = \frac{1}{f_{\mathrm{ref}}(\lambda)} + \frac{1}{f_{\mathrm{dif}}(\lambda)} \tag{4}$$

3.2. Achromatization

Because f_{eff} depends on the wavelength and solar spectrum varies widely, the LCA of the hybrid lens hinders light harvesting. The Abbe number is usually used to measure the dispersion in the visible region [15, 19]. Considering the typical absorption spec-

trum of organic active materials is from 360 to 900 nm, we introduce the OSC Abbe number of a refractive lens

$$v_{\text{ref, OSC}} = \frac{n(\lambda_2) - 1}{n(\lambda_1) - n(\lambda_3)} \tag{5}$$

where $\lambda_1 < \lambda_2 < \lambda_3$, λ_1 and λ_2 are the minimum and maximum wavelength within the absorption spectrum of an active material, respectively. Similarly, the OSC Abbe number of a diffractive lens

$$v_{\text{dif, OSC}} = \frac{\lambda_2}{\lambda_1 - \lambda_3} \tag{6}$$

Therefore, for an achromatic design of the hybrid lens, f_{ref} and f_{dif} mentioned above must meet the longitudinal achromatization condition

$$f_{\text{ref}} v_{\text{ref, OSC}} + f_{\text{dif}} v_{\text{dif, OSC}} = 0 \tag{7}$$

3.3. Hole parameter design

The appropriate size and position of holes can allow the spectrum of interest to pass through, and restrict part of other incident light which is unable to be absorbed or harmful to organic materials. So the hole parameters must be optimized for trapping light. As shows in Fig. 3, the best distance z_0 from the hybrid lens to the mirror is given by the intersection of two lines, $x_1(z)$ and $x_2(z)$. The straight line equations are given respectively by

$$x_1(z) = -\frac{D}{2(f_0 + \Delta)} z + \frac{D}{2} \tag{8}$$

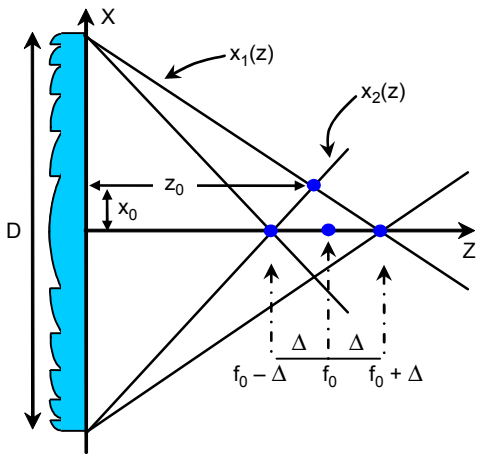

Fig. 3. Schematic diagram of the hole parameter analysis.

$$x_2(z) = \frac{D}{2(f_0 - \Delta)} z - \frac{D}{2} \tag{9}$$

where D is the diameter of the lens, Δ is the LCA of the lens, and the average effective focal length f_0 is the median of the minimum f_{eff} and the maximum f_{eff} within the design wavelength range.

Thus, the z-coordinate of the intersection representing the best distance is given by

$$-\frac{D}{2(f_0 + \Delta)} z_0 + \frac{D}{2} = \frac{D}{2(f_0 - \Delta)} z_0 - \frac{D}{2} \tag{10}$$

so

$$z_0 = f_0 \left(1 - \frac{\Delta^2}{f_0^2} \right) \tag{11}$$

The x-coordinate of the intersection representing the best radius of the hole is given by

$$x_0 = -\frac{D}{2(f_0 + \Delta)} z_0 + \frac{D}{2} = -\frac{D}{2(f_0 + \Delta)} \left(f_0 - \frac{\Delta^2}{f_0} \right) + \frac{D}{2} = \frac{D}{2} \frac{\Delta}{f_0} \tag{12}$$

So the best diameter d_0 of the hole (Fig. 3) is given by

$$d_0 = 2x_0 = D \frac{\Delta}{f_0} \tag{13}$$

For easy comparison, the best relative aperture d_0^* of the hole is introduced

$$d_0^* = \frac{d_0}{D} = \frac{\Delta}{f_0} \tag{14}$$

Thus, Eq. (11) can be rewritten as

$$z_0 = f_0 \left(1 - \frac{\Delta^2}{f_0^2} \right) = f_0 \left[1 - (d_0^*)^2 \right] \tag{15}$$

It is obvious that $(d_0^*)^2$ is greater than zero, so z_0 is always smaller than f_0.

4. Results and discussion

The f_{eff} of a hybrid lens is given by Eq. (4), but the achromatization condition (Eq. (7)) determines the power allocation. So when the desired focal length $f_{0_{\text{eff}}}$ is selected, the theoretical values of f_{ref} and f_{dif} at the design wavelength λ_0 can be obtained according to Eqs. (4)–(7). In the following simulations, $f_{0_{\text{eff}}}$ is always fixed at 1000 μm for comparison.

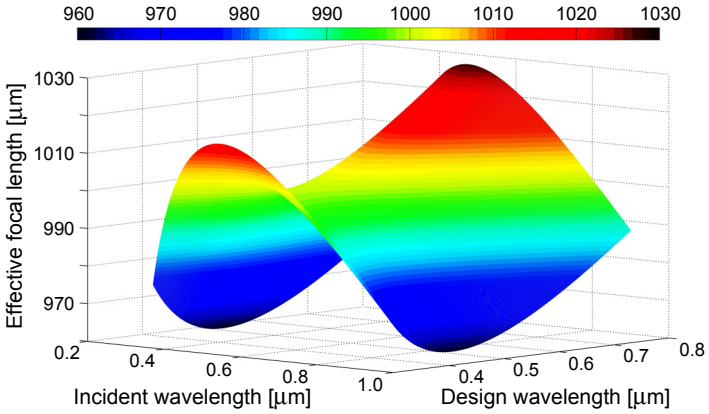

Fig. 4. Effective focal length f_{eff} of a hybrid microlens as functions of incident wavelength and design wavelength ($f_{0_{\text{eff}}}$ = 1000 μm).

Considering the material dispersion, for example, the typical refractive index of PMMA varies from 1.52 to 1.47 (Fig. 2), f_{eff} of the hybrid lens varies with wavelength. Figure 4 shows f_{eff} as functions of incident wavelength and design wavelength. The simulation result reveals that achromatism occurs only at certain wavelengths in the condition of widely incident spectrum, so f_{eff} depends not only on incident wavelength, but also on design wavelength. In addition, the saddle-shaped surface in this figure indicates that f_{eff} is a non-monotonic function of wavelength, and LCA can be optimized by the focal length design and the absorption spectrum of active materials. So the achromatic and focusing properties of the hybrid microlens should be analyzed carefully in order to acquire optimal achromatic condition and optimal light management.

As previously mentioned in Section 2.1, if a converging lens replaces the hybrid lens in this lighting trapping system, the large chromatic aberration of the refractive

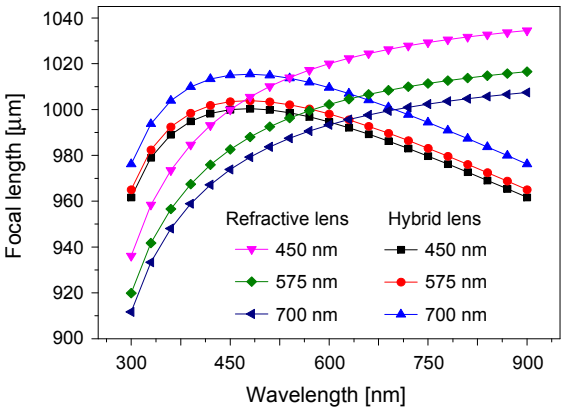

Fig. 5. The comparison of focal lengths between refractive lenses and hybrid lenses at design wavelengths ($f_{0_{\text{eff}}}$ = 1000 μm).

lens will impede light harvesting. Figure 5 shows the comparison of the focal length between refractive lenses and hybrid microlenses at different design wavelengths. This plot consists of two sets of curves which respectively represent the focal length of the hybrid lens and refractive lens. The legends illustrate design wavelengths of each set of curves, 450, 575 and 700 nm. In other words, $f_{0\text{eff}}$ at these wavelengths is always 1000 μm. It is obvious that Fig. 5 shows significant difference between the two sets of curves. The curves of refractive lenses monotonically increase with wavelength, but those of hybrids lenses increase firstly with wavelength, reach maximums and then decline. It is the curve feature of firstly increasing then decreasing that proves the LCA of hybrid lenses to be obviously smaller than refractive lenses. Further analysis reveals that the LCA of hybrid lenses is about 2.5 times less than refractive lenses. Therefore, the hybrid lens array proposed in this work can achieve excellent achromatism and light trapping comparing with the refractive lens array.

The mirror with holes is one of key elements in lighting trapping scheme, the appropriate size and position of holes are important to harvest the light beam converged by hybrid lenses. If the hole is too close or too far away from the hybrid lens, a part of convergent light cannot pass through the hole, so this part of light cannot be absorbed by the active layer. Similarly, too big or too small size is also a disadvantage for light trapping, because convergent light will be partly blocked by too small hole, and the reflected rays coming from the reflecting electrode will escape form too big hole. Figure 6 shows the best hole position at different design wavelengths. It is interesting that the curve variation tendencies of hybrid lenses in Fig. 6 are just opposite to those in Fig. 5, so also behave the curves of refractive lenses in the two figures. Figure 6 indicates that though $f_{0\text{eff}}$ is a fixed value, the best position is not constant but changes with the design wavelength. Note that the minimum value of the hybrid lens curve is not the optimum position in the whole wavelength range. The optimum position of a hole for the whole light trapping scheme is not only the best position at a certain design wavelength, but also for the absorption spectrum of an active layer. In addition, this figure also illustrates that the LCA of refractive lens is larger than hybrid lens.

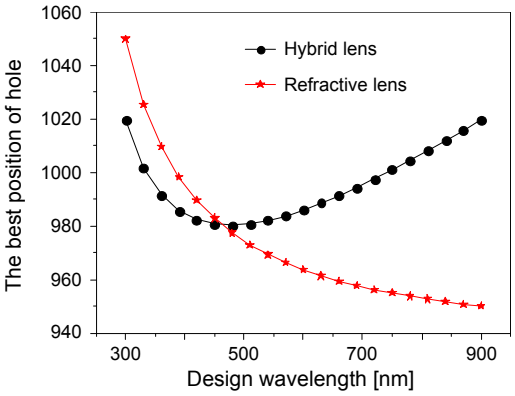

Fig. 6. The best positions of a hole at design wavelengths ($f_{0\text{eff}}$ = 1000 μm).

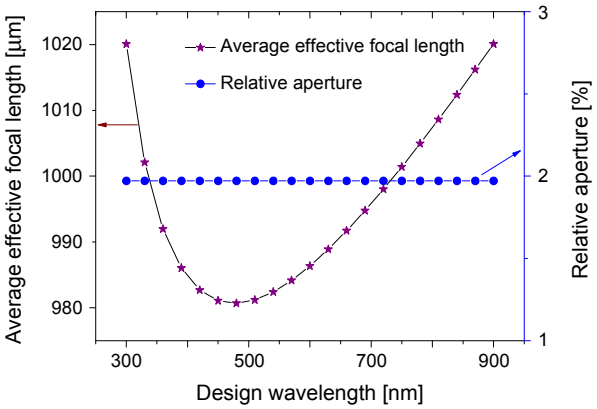

Fig. 7. The average effective focal lengths of hybrid lens and the relative aperture of hole at design wavelengths ($f_{0_{\text{eff}}}$ = 1000 μm).

The diameter is another important parameter of the hole. Here the relative aperture is introduced and is defined by Eq. (14). For easy comparison, Fig. 7 shows the relative aperture $d_0^*(\lambda)$ and the average effective focal length $f_0(\lambda)$ of hybrid lens. Though $d_0^*(\lambda)$ shown in this figure is constant within the design wavelength range, this does not mean that a certain hole diameter is always suitable for all design wavelengths. Actually, the LCA and $f_0(\lambda)$ also change with design wavelength, but only the ratio of LCA to $f_0(\lambda)$ does not vary with design wavelength. At the same time, it is easy to find that the curve of the best position (Fig. 6) is similar to $f_0(\lambda)$ (Fig. 7). In fact, there is only a slight difference between the two curves. It is easy to see from Eq. (15) that the best position $z_0(\lambda)$ is always smaller than the average effective focal length $f_0(\lambda)$ at the same design wavelength. For a hybrid lens of PMMA, the relative aperture d_0^* is usually about 2% (see Fig. 7). So $z_0(\lambda)$ is slightly less than $f_0(\lambda)$, the difference is less than 1% in our case. Therefore, to simplify the design process, $f_0(\lambda)$ can be regarded as the best hole position. As for the best hole size, it also needs the optimal design according to the absorption spectrum of active materials and achromatization condition.

5. Conclusions

A highly efficient light trapping scheme is proposed to enhance broadband absorption in OSC, which bases on a hybrid microlens array and a mirror with hole array. By comparing the effective focal length, best hole position and size in the two types of lenses (the refractive lens and the hybrid lens), the hybrid lens has more excellent light trapping ability due to the lesser LCA. The simulation results also indicate that the hybrid lens can be further optimized with the achromatization condition and the absorption spectrum of an active layer, and the average effective focal length can be regarded as the best hole position for simplifying the design process. In short, this scheme can ef-

fectively enhance light absorption in the spectrum of interest by chromatic aberration correction and hole parameter adjustment, and it is separated from cells to avoid direct contact with organic layer that maybe cause electrical defects, moreover can be made by low cost manufacturing technologies such as imprint.

Acknowledgements – This work was supported by the Nation Natural Science Foundations (Nos. 11305111, 61377050 and 61307039), International Cooperation and Exchange of Science and Technology Project in Sichuan Province (No. 2013HH0010), Collaborative Innovation Foundation (No. XTCX 2013002), and the Natural Science Foundations of Leshan Normal University.

References

[1] Minh Trung Dang, Hirsch L., Wantz G., Wuest J.D., *Controlling the morphology and performance of bulk heterojunctions in solar sells. Lessons learned from the benchmark poly(3-hexylthiophene): [6, 6]-phenyl-C_{61}-butyric acid methyl ester system*, Chemical Reviews **113**(5), 2013, pp. 3734–3765.

[2] Qi Wu, Bhattacharya M., Morgan S.E., *POSS-enhanced phase separation in air-processed P3HT:PCBM bulk heterojunction photovoltaic systems*, ACS Applied Materials and Interfaces **5**(13), 2013, pp. 6136–6146.

[3] Pfannmöller M., Kowalskybc W., Schröder R.R., *Visualizing physical, electronic, and optical properties of organic photovoltaic cells*, Energy and Environmental Science **6**(10), 2013, pp. 2871–2891.

[4] Sondergaard R., Hösel M., Angmo D., Larsen-Olsen T.T., Krebs F.C., *Roll-to-roll fabrication of polymer solar cells*, Materials Today **15**(1–2), 2012, pp. 36–49.

[5] Doo-Hyun Ko, Tumbleston J.R., Gadisa A., Aryal M., Yingchi Liu, Lopez R., Samulski E.T., *Light-trapping nano-structures in organic photovoltaic cells*, Journal of Materials Chemistry **21**(41), 2011, pp. 16293–16303.

[6] Vynck K., Burresi M., Riboli F., Wiersma D.S., *Photon management in two-dimensional disordered media*, Nature Materials **11**(12), 2012, pp. 1017–1022.

[7] Xuanhua Li, Wallace Chik Ho Choy, Haifei Lu, Wei E.I. Sha, Aaron Ho Pui Ho, *Efficiency enhancement of organic solar cells by using shape-dependent broadband plasmonic absorption in metallic nanoparticles*, Advanced Functional Materials **23**(21), 2013, pp. 2728–2735.

[8] Luzhou Chen, Wei E.I. Sha, Wallace C.H. Choy, *Light harvesting improvement of organic solar cells with self-enhanced active layer designs*, Optics Express **20**(7), 2012, pp. 8175–8185.

[9] Sergeant N.P., Niesen B., Liu A.S., Boman L., Stoessel C., Heremans P., Peumans P., Rand B.P., Shanhui Fan, *Resonant cavity enhanced light harvesting in flexible thin-film organic solar cells*, Optics Letters **38**(9), 2013, pp. 1431–1433.

[10] Ducheé D., Drouard E., Simon J.J., Escoubas L., Torchio Ph., Le Rouzo J., Vedraine S., *Light harvesting in organic solar cells*, Solar Energy Materials and Solar Cells **95**(S1), 2011, pp. S18–S25.

[11] Yidong Hou, Shuhong Li, Song Ye, Sha Shi, Maoguo Zhang, Ruiying Shi, Jinglei Du, Chunlei Du, *Using self-assembly technology to fabricate silver particle array for organic photovoltaic devices*, Microelectronic Engineering **98**, 2012, pp. 428–432.

[12] Tvingstedt K., Dal Zilio S., Inganäs O., Tormen M., *Trapping light with micro lenses in thin film organic photovoltaic cells*, Optics Express **16**(26), 2008, pp. 21608–21615.

[13] Zilio S.D., Tvingstedt K., Inganäs O., M. Tormen, *Fabrication of a light trapping system for organic solar cells*, Microelectronic Engineering **86**(4–6), 2009, pp. 1150–1154.

[14] Languy F., Fleury K., Lenaerts C., Loicq J., Regaert D., Thibert T., Habraken S., *Flat Fresnel doublets made of PMMA and PC: combining low cost production and very high concentration ratio for CPV*, Optics Express **19**(S3), 2011, pp. A280–A294.

[15] LANGUY F., LENAERTS C., LOICQ J., THIBERT T., HABRAKEN S., *Performance of solar concentrator made of an achromatic Fresnel doublet measured with a continuous solar simulator and comparison with a singlet*, Solar Energy Materials and Solar Cells **109**, 2013, pp. 70–76.
[16] KHAI Q. LE, ABASS A., MAES B., BIENSTMAN P., ALU A., *Comparing plasmonic and dielectric gratings for absorption enhancement in thin-film organic solar cells*, Optics Express **20**(S1), 2012, pp. A39–A50.
[17] SULTANOVA N., KASAROVA S., NIKOLOV I., *Dispersion properties of optical polymers*, Acta Physica Polonica A **116**(4), 2009, pp. 585–587.
[18] MORENO V., ROMÁN J.F., SALGUEIRO J.R., *High efficiency diffractive lenses: deduction of kinoform profile*, American Journal of Physics **65**(6), 1997, pp. 556–562.
[19] DAVIDSON N., FRIESEM A.A., HASMAN E., *Analytic design of hybrid diffractive-refractive achromats*, Applied Optics **32**(25), 1993, pp. 4770–4774.

Received June 10, 2014
in revised form January 13, 2015